BETACOOL Code Development and Beam Dynamics Simulations

Final report

to the ANNEX NO. 1

of the Memorandum of Understanding between

Gesellschaft für Schwerionenforschung mbH (GSI), Darmstadt, Germany

and

Joint Institute for Nuclear Research (JINR), Dubna, Russia

dated March 2006

I.N.Meshkov, R.V. Pivin, A.O. Sidorin, A.V.Smirnov, G.V.Trubnikov
Joint Institute for Nuclear Research, Dubna, Russia

October 2006

Abstract

This report summarizes results of the software development during the Contract realization from March 1, 2006 to November 1, 2006. As it was agreed JINR made available to GSI a manual of the special program version and the results of beam simulations.

General attention at this stage of the work was devoted to development of the electron cooling models in order to provide realistic comparison between new implemented cooling force calculation (model by Erlangen), new target model and experiments at GSI ESR ring. New model of electron beam – hollow beam was introduced for providing simulations for possible regimes of future HESR. New algorithms for calculation of the electron cooling friction force and internal target (so-called fiber jet) for more realistic simulations were implemented. A new model of IBS calculation – which was created by O.Boine-Frankenheim and P.Zenkevich - kinetic simulation of IBS process which presumes a solution of Langevin equation for each model particle.
A special dedicated version for GSI was created with only necessary options for calculations and user manual.

Contents

SUMMARY OF CODE DEVELOPMENT

Initial design of RHIC electron cooling system presumed generation of magnetized electron beam and its injection after acceleration into solenoid providing longitudinal magnetic field of the value of 2 – 5 T. Large emittance of the electron beam prevents ion-electron recombination in the cooling section and electron magnetization provides large enough cooling force.

Within the framework of the above-mentioned agreement, JINR and GSI worked together to study beam parameters in the storage rings CR, RESR, NESR and HESR of the FAIR project. The work successfully covered in this attachment was the following:

- Provision of a special version of the BETACOOL code according to the specific requirements of the FAIR project. This included
  - Implementation of the cooling force model by Ch. Töpffer
  - The option of hollow electron beams
  - The interaction with internal gas and pellet targets.
- Benchmarking of the BETACOOL code in cooperation with GSI which is performing experiments on cooling and the influence of an internal target
- JINR participation in the studies of beam parameters in the various FAIR storage ring on the basis of the present design of the cooling systems

A manual of the special program version and the results of beam simulations are available to GSI.

A few models for magnetized cooling simulation were developed in the frame of previous contracts between GSI and JINR. The results of the magnetized friction force calculation were compared with experimental results of ESR experiments. As result the accuracy of the cooling rate calculation was increased and disagreement between numerical models and experimental results does not exceed 50%. For now a new model of friction force calculation was added to the code – model developed by group from Erlangen University. This model covers all ranges of binary collisions – fast (non-magnetized) and two options for magnetized interaction – so called stretched helices and tight helices.

Obvious advantages of non-magnetized version of the cooler design stimulate development and benchmarking of the algorithm for cooling force calculation in absence of the magnetic field. In previous version of BETACOOL program for friction force calculation in nonmagnetized electron beam the following algorithms were used:
- numerical evaluation of 3D integral over the electron distribution function in the case of flattened velocity distribution,
- Chandrasekhar's formula for the friction force at uniform Maxwellian velocity distribution,
- Asymptotic formulae for the friction force at flattened velocity distribution derived by Meshkov.

To provide accurate benchmarking of the existing algorithms and to improve accuracy and speed of the calculation two new algorithms were introduced into the code: Binney's formula and asymptotic representation by Derbenev for flattened velocity distribution and new binary collision model for friction force derived by Erlangen.

Benchmarking of new Erlangen model with experimental data showed rather high accuracy of new friction force model and its more close coincidence to experimental results in comparison with magnetized model (Derbenev-Meshkov-Skrinsky), Parkhomchuk model and non-magnetized.

Kinetic simulation of IBS process presumes a solution of Langevin equation for each model particle. The drift and diffusion terms of the equation has to be calculated for each particle independently

as a function of its co-ordinates, velocity components and distribution function of all other particles in the Model Beam.

To benchmark the algorithm reducing friction and diffusion to Langevin force components the simplified kinetic model for IBS simulation proposed by P.Zenkevich and O.Boine-Frankenheim was introduced into the code and tested preliminary at parameters typical for gold-gold collisions at RHIC. This model is based on analytical formulae for friction and diffusion components and presumes that only the friction depends on the particle velocity. The diffusion tensor in the frame of this model does not depend on the particle momentum and has a simplified structure.

Benchmarking of new model of internal target – fiber jet (proposed and derived by A.Sidorin) - with experimental results from GSI ESR and with very sophisticated Kiev model showed its very good efficiency, close coincidence to experimental results and its applicability and convenience for long-term beam heating and cooling processes simulation.

Description of all developed new models for different effects and algorithms are presented in this summary. New user manual for dedicated GSI BETACOOL version was also created and included to this report.

1. MODEL OF ELECTRON COOLING FRICTION FORCE DEVELOPED BY ERLANGEN UNIVERSITY.

1.1. Erlangen model formalism

In [B.Mollers et al, Drag force on ions in magnetized electron plasmas, NIM B 207 (2003) 462-481] the friction force was calculated in the frame of binary collision model under assumption that the ion velocity stays constant in a collision with an electron. The unperturbed motion of electron is a helix with the Larmor radius:

$$\rho_\perp = \frac{cmv_\perp}{eB} \tag{1.1}$$

and the pitch determined by longitudinal velocity. The ion velocity variation is calculated iteratively and at impact parameters larger than the Larmor radius one can obtain solution in a closed form for two limiting cases:

$$\delta = \frac{cm\sqrt{V_\perp^2 + \left(V_\parallel - v_\parallel\right)^2}}{eB} >> \rho_\perp$$

and $\delta << \rho_\perp$, where δ is the pitch of the helix as seen from the ion.

Correspondingly, the friction force includes three components related to different types of collision:

- fast collisions at impact parameters less than radius of electron rotation,
- collisions with “tight” helices,
- collisions with “stretched” helices.

In the case of axial symmetry the electron distribution function can be written in the following form:

$$f\left(v_e\right) = \left(\frac{1}{2\pi}\right)^{3/2} \frac{1}{\Delta_\perp^2 \Delta_\parallel} \exp\left(-\frac{v_\perp^2}{2\Delta_\perp^2} - \frac{v_\parallel^2}{2\Delta_\parallel^2}\right), \tag{1.2}$$

where $\Delta_\perp$ and $\Delta_\parallel$ are the electron rms velocity spreads in the transverse and longitudinal direction correspondingly.

For the fast collisions the formula is analogous to non-magnetized collisions. The components of the friction force at fast collisions can be calculated in cylindrical co-ordinate system as follows:

$$F_{\perp,f} = -\sqrt{\frac{2}{\pi}} \frac{Z^2 e^4 n_e}{m\Delta_\perp^2 \Delta_\parallel} \int_0^\infty \int_{-\infty}^\infty \int_0^{2\pi} \ln\left(\frac{\rho_{\max}}{\rho_{\min}}\right) \frac{\left(V_\perp - v_\perp \cos\varphi\right) \exp\left(-\frac{v_\perp^2}{2\Delta_\perp^2} - \frac{v_\parallel^2}{2\Delta_\parallel^2}\right)}{\left(\left(V_\parallel - v_\parallel\right)^2 + \left(V_\perp - v_\perp \cos\varphi\right)^2 + v_\perp^2 \sin^2\varphi\right)^{3/2}} v_\perp d\varphi dv_\parallel dv_\perp ,$$

$$F_{\parallel,f} = -\sqrt{\frac{2}{\pi}} \frac{Z^2 e^4 n_e}{m\Delta_\perp^2 \Delta_\parallel} \int_0^\infty \int_{-\infty}^\infty \int_0^{2\pi} \ln\left(\frac{\rho_{\max}}{\rho_{\min}}\right) \frac{\left(V_\parallel - v_\parallel\right) \exp\left(-\frac{v_\perp^2}{2\Delta_\perp^2} - \frac{v_\parallel^2}{2\Delta_\parallel^2}\right)}{\left(\left(V_\parallel - v_\parallel\right)^2 + \left(V_\perp - v_\perp \cos\varphi\right)^2 + v_\perp^2 \sin^2\varphi\right)^{3/2}} v_\perp d\varphi dv_\parallel dv_\perp . \tag{1.3}$$

But here both impact parameters – minimum and maximum – are the functions of the electron velocity:

$$\rho_{\min} = \frac{Ze^2}{m_e} \frac{1}{\left(V_\parallel - v_\parallel\right)^2 + \left(V_\perp - v_\perp \cos\varphi\right)^2 + v_\perp^2 \sin^2\varphi} . \tag{1.4}$$

$$\rho_{\max} = \rho_{\perp} = \frac{cmv_{\perp}}{eB}.$$

The friction force in collisions with tight helices

$$F_{\parallel,t}\left(V_{\perp},V_{\parallel}\right) = -\frac{4\pi Z^2 e^4 n_e}{m}\frac{1}{\Delta_{\perp}^2\sqrt{2\pi}\Delta_{\parallel}}\int\frac{V_{\perp}^2\left(V_{\parallel}-v_{\parallel}\right)}{\left(V_{\perp}^2+\left(V_{\parallel}-v_{\parallel}\right)^2\right)^{5/2}}\exp\left(-\frac{v_{\parallel}^2}{2\Delta_{\parallel}^2}\right)$$
$$\int_0^{\infty}\ln\left(\frac{\rho_{\max}}{\max\left(\rho_{\perp},\delta\right)}\right)\exp\left(-\frac{v_{\perp}^2}{2\Delta_{\perp}^2}\right)v_{\perp}dv_{\perp}dv_{\parallel}, \qquad (1.5)$$

$$F_{\perp,t}\left(V_{\perp},V_{\parallel}\right) = -\frac{4\pi Z^2 e^4 n_e}{m}\frac{1}{\Delta_{\perp}^2\sqrt{2\pi}\Delta_{\parallel}}\int\frac{V_{\perp}\left(V_{\perp}^2-\left(V_{\parallel}-v_{\parallel}\right)^2\right)}{2\left(V_{\perp}^2+\left(V_{\parallel}-v_{\parallel}\right)^2\right)^{5/2}}\exp\left(-\frac{v_{\parallel}^2}{2\Delta_{\parallel}^2}\right)$$
$$\int_0^{\infty}\ln\left(\frac{\rho_{\max}}{\max\left(\rho_{\perp},\delta\right)}\right)\exp\left(-\frac{v_{\perp}^2}{2\Delta_{\perp}^2}\right)v_{\perp}dv_{\perp}dv_{\parallel}, \qquad (1.6)$$

where

$$\delta = \frac{cm\sqrt{V_{\perp}^2+\left(V_{\parallel}-v_{\parallel}\right)^2}}{eB}. \qquad (1.7)$$

For stretched helices

$$F_{\parallel,s}\left(V_{\perp},V_{\parallel}\right) = -\frac{4\pi Z^2 e^4 n_e}{m}\frac{1}{\Delta_{\perp}^2\sqrt{2\pi}\Delta_{\parallel}}\int\frac{V_{\parallel}-v_{\parallel}}{\left(V_{\perp}^2+\left(V_{\parallel}-v_{\parallel}\right)^2\right)^{3/2}}\exp\left(-\frac{v_{\parallel}^2}{2\Delta_{\parallel}^2}\right)$$
$$\int_0^{\infty}\ln\left(\frac{\min(\delta,\rho_{\max})}{\min\left(\rho_{\perp},\rho_{\max}\right)}\right)\exp\left(-\frac{v_{\perp}^2}{2\Delta_{\perp}^2}\right)v_{\perp}dv_{\perp}dv_{\parallel}, \qquad (1.8)$$

$$F_{\perp,s}\left(V_{\perp},V_{\parallel}\right) = -\frac{4\pi Z^2 e^4 n_e}{m}\frac{V_{\perp}}{\Delta_{\perp}^2\sqrt{2\pi}\Delta_{\parallel}}\int\frac{1}{\left(V_{\perp}^2+\left(V_{\parallel}-v_{\parallel}\right)^2\right)^{3/2}}\exp\left(-\frac{v_{\parallel}^2}{2\Delta_{\parallel}^2}\right)$$
$$\int_0^{\infty}\ln\left(\frac{\min(\delta,\rho_{\max})}{\min\left(\rho_{\perp},\rho_{\max}\right)}\right)\exp\left(-\frac{v_{\perp}^2}{2\Delta_{\perp}^2}\right)v_{\perp}dv_{\perp}dv_{\parallel}. \qquad (1.9)$$

When V >> $\Delta_{\parallel}$ the electron distribution can be approximated by delta-function $f\left(v_{\parallel}\right)=\delta\left(v_{\parallel}\right)$. In this case integration over electron velocity components can be provided independently. The friction force components for tight helices can be expressed in the following form:

$$F_{\parallel} = -V_{\parallel}\frac{4\pi Z^2 e^4 n_e}{mV^3}\frac{V_{\perp}^2}{V^2}L_M, \qquad (1.10)$$

$$F_{\perp} = -V_{\perp}\frac{4\pi Z^2 e^4 n_e L_M}{mV^3}\frac{V_{\perp}^2-V_{\parallel}^2}{V^2}. \qquad (1.11)$$

Here the Coulomb logarithm is determined by the expression

$$L_M = \frac{1}{\Delta_{\perp}^2}\int_0^{\infty}\ln\left(\frac{\rho_{\max}}{\max\left(\rho_{\perp},\delta\right)}\right)\exp\left(-\frac{v_{\perp}^2}{2\Delta_{\perp}^2}\right)v_{\perp}dv_{\perp} \approx \ln\left(\frac{\rho_{\max}}{\langle\rho_{\perp}\rangle}\right),$$

at $\delta = \frac{cm\sqrt{V_\perp^2 + V_\parallel^2}}{eB}$. Within an accuracy to the logarithm definition these formulae coincide with derived in the limit of infinite magnetic field in [doctoral thesis by V.Parkhomchuk].

In the same approximation $V >> \Delta_\parallel$ the formulae for collisions with stretched helices can be rewritten in the form:

$$\overset{\circ}{F} \approx -\overset{\circ}{V}\frac{4\pi Z^2 e^4 n_e}{m}\frac{1}{\left(V^2+\Delta_\parallel^2\right)^{3/2}}\left(\ln\left(\frac{\rho_{max}}{\langle\rho_\perp\rangle}\right)+\ln\left(\frac{\omega_p}{\omega_B}\right)\right), \qquad (1.12)$$

where ω_p, ω_B are the plasma and cyclotron frequencies. This formula is valid at $\frac{V}{\Delta_\perp} >> 1$ and its structure is similar to semi-empirical formula by Parkhomchuk.

Numerical integration of (5) has to be provided taking into account peculiarity of the integral at $V_\perp \to 0$.

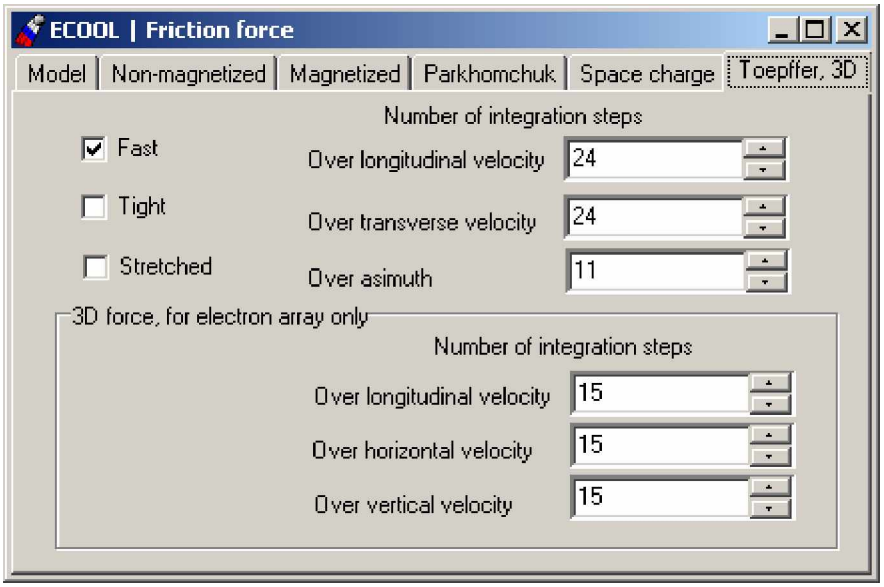

Fig. 1.1. Visual form for input parameters of Toepffer and 3D friction force calculation.

1.2. Benchmarking the code

Some study was dedicated to the optimization of the table size and splitting :

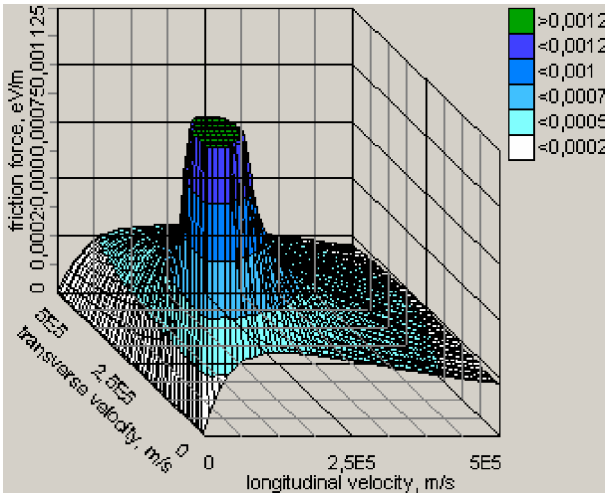

Longitudinal friction force component

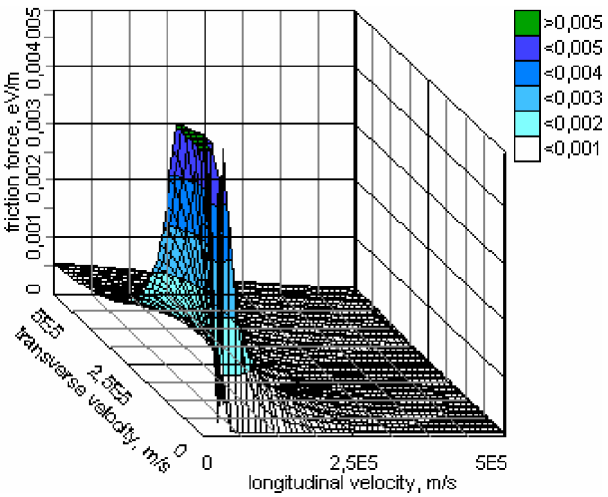

Transverse Friction force component

$F_{\perp}$ component	$F_{\parallel}$ component
$V_{\perp}$ (m/s) From 0 to 20.000 – 2 steps 20.000 – 200.000 – 6 steps 200.000 – 500.000 – 1 step	$V_{\perp}$ (m/s) From 0 to 20.000 – 2 steps 20.000 – 200.000 – 6 steps 200.000 – 500.000 – 1 step
$V_{\parallel}$ (m/s) From 0 to 20.000 – 2 steps 20.000 – 150.000 – 6 steps 150.000 – 500.000 – 1 step	$V_{\parallel}$ (m/s) From 0 to 30.000 – 2 steps 30.000 – 250.000 – 6 steps 250.000 – 500.000 – 1 step

ESR ring, 400 MeV/u, A = 208, Z = 82, C = 108.36 m, Tune_h = Tune_v = 2.3 , RF harmonic number = 1, RF = 5 kV, standard ESR lattice, coasting beam, ε_h = ε_v = 0.3 pi-mm-mrad, dP/P = 0.0002, N_p = 1.5e8.

ECOOL parameters: L_cooler = 1.8 m, B = 1 kG, β_h = 16 m, β_v = 6.9 m, α, D, D'– zero, Uniform cylinder, r_e = 2,5 cm, $T_{\perp}$ = 0.1eV, $T_{\parallel}$ = 0.0001 eV.

Simulations were provided for different values of the electron beam current (from 0,05 to 0,8 A) – to compare with experimental data and simulation made with other friction force models.

Here ***Erlan Analit*** – implemented algorithm into BETAACOOL code, based on "Erlangen" theory, but with little modifications (to fasten calculation). ***Erlan.Table*** – simulations were made with using values from pre-calculated friction force tables. Tables are obtained by Erlangen group and calculated with their program code for definite storage rings parameters (ESR with different electron beam current values). ***Erlan pure*** – simulations made with BETACOOL but in this case algorithm is absolutely identical to the theory developed by Erlangen (with no modifications).

We expect that difference between Erlan Pure/An and Erlan Tab can be explained by two reasons. The main reason is connected with the situation when one uses table of friction force values for calculation it is necessary to interpolate (user can choose – linear interpolation or bilinear which is more precise), and small divergence in result is explained by interpolation error and it's method. The second reason for difference is probably the grid of the table and a range of velocities for which the friction force mesh is built. Actually we would advise to use a possibility of table making when you can organize three ranges of velocity and generate friction force values within every range with different splitting.

Simulations for ESR

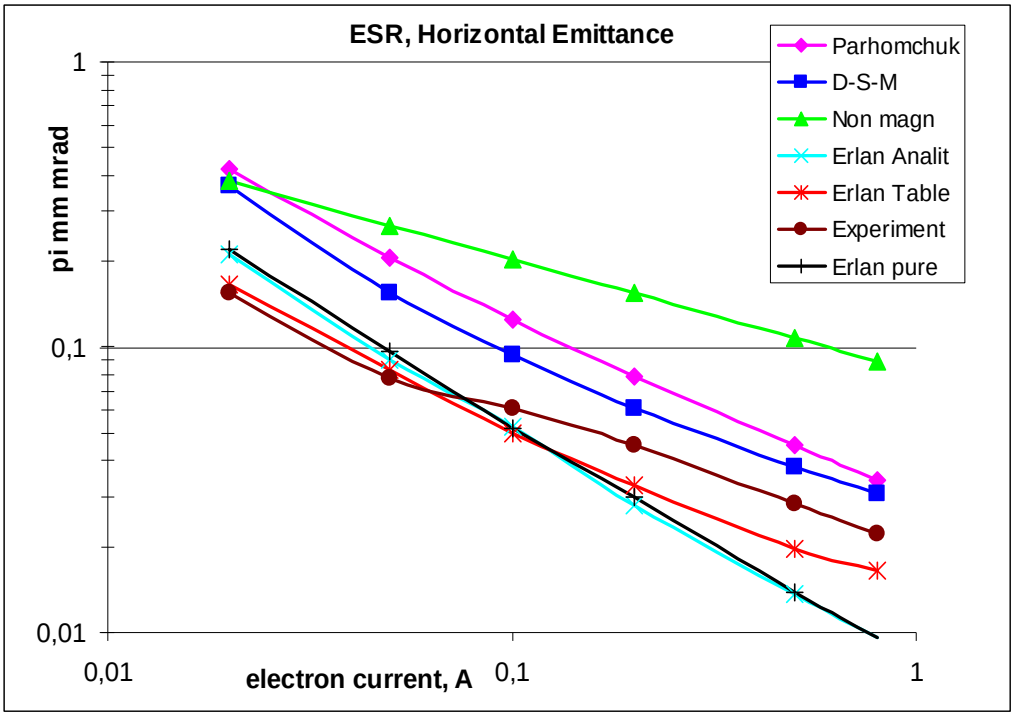

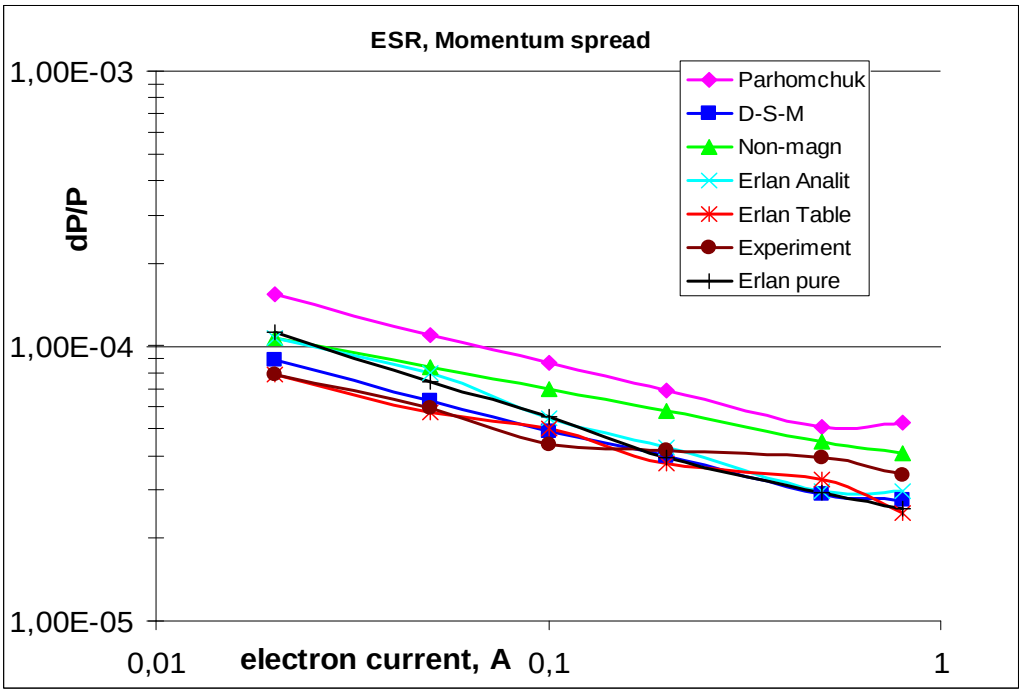

Simulations for HESR

In simulations were modeled HESR regime with high luminosity when it is necessary to get beam with momentum spread of order of 1e-5.. That's why were compared equilibrium parameters obtained with Parhomchuk formula, Derbenev-Skrinsky-Meshkov (D-S-M) for magnetized cooling, and new implemented models of friction force calculation – theory by Erlangen group. We tested (for inside checking) simultaneously both Erlangen models – first one calculates analytically using algorithm implemented to program code BETACOOL (on plots – Erlangen An), the other – tables calculated by Erlangen with their own code for the defined parameters of the storage ring (on plots – Erlangen Tab).
As had shown calculation it is more efficient to use Tabulated friction force in case of HESR because for calculation of equilibrium (if IBS and ECOOL effects are switched ON) by Erlangen model (Analitical) it requires several hours to calculate every point on the plot. In case of using pre-calculated table it takes only several minutes.
As a result from calculations one can say that if take Erlangen model for HESR HL regime simulation then equilibrium shifts to the region of less momentum spread and emittances. Actually it is easily seen from formulae – Erlangen theory gives approximately 2 times higher longitudinal cooling rate and higher transverse cooling rate in comparison say to Parhomchuk theory.
Also simulations were provided for different values of the magnetic filed in cooler. Results shown that magnetic field value does not influence on the final equilibrium.

Ring parameters:
HESR ring, 8 GeV, protons, circ. 574,0216m, hor.tune = vert.tune = 12,17, RF harmonic number = 90, RF voltage = 450 kV, standard HESR lattice (given by GSI), coasting beam, emittance_hor = emittance_vert = 0,08 pi-mm-mrad, dP/P = 3,5e-5, Number_protons = 1e10.
ECOOL parameters:
L_cooler = 15m, B_field = 2 kG, beta_hor = beta_vert = 100m, alphas, dispersions, D's – zero.
Electron beam – uniform cylinder, beam radius = 0,5 cm, beam current 0,1 A, transverse_temperature = 1eV, long_temp = 0,001 eV.

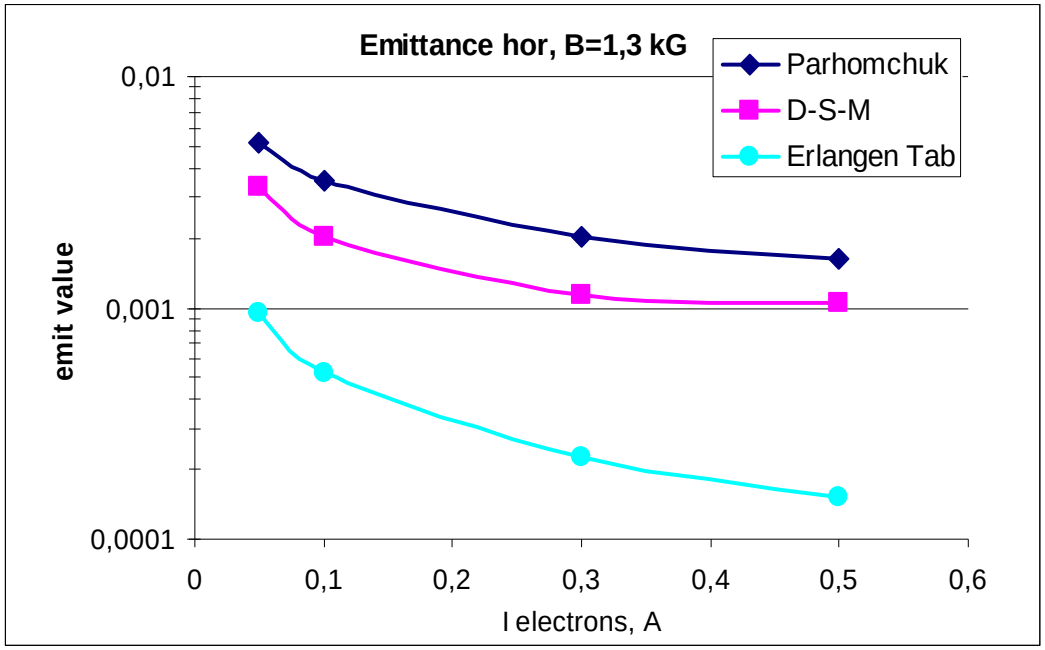
Emittance hor, B=1,3 kG
Parhomchuk
D-S-M
Erlangen Tab
emit value
0,01
0,001
0,0001
0
0,1
0,2
0,3
0,4
0,5
0,6
I electrons, A

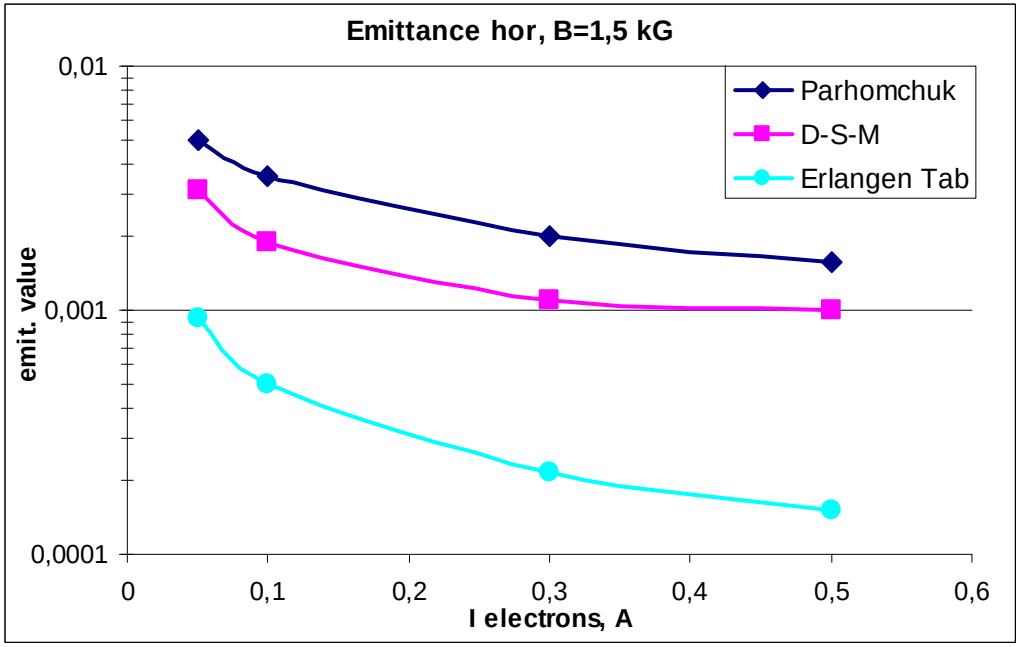
Emittance hor, B=1,5 kG
Parhomchuk
D-S-M
Erlangen Tab
emit. value
0,01
0,001
0,0001
0
0,1
0,2
0,3
0,4
0,5
0,6
I electrons, A

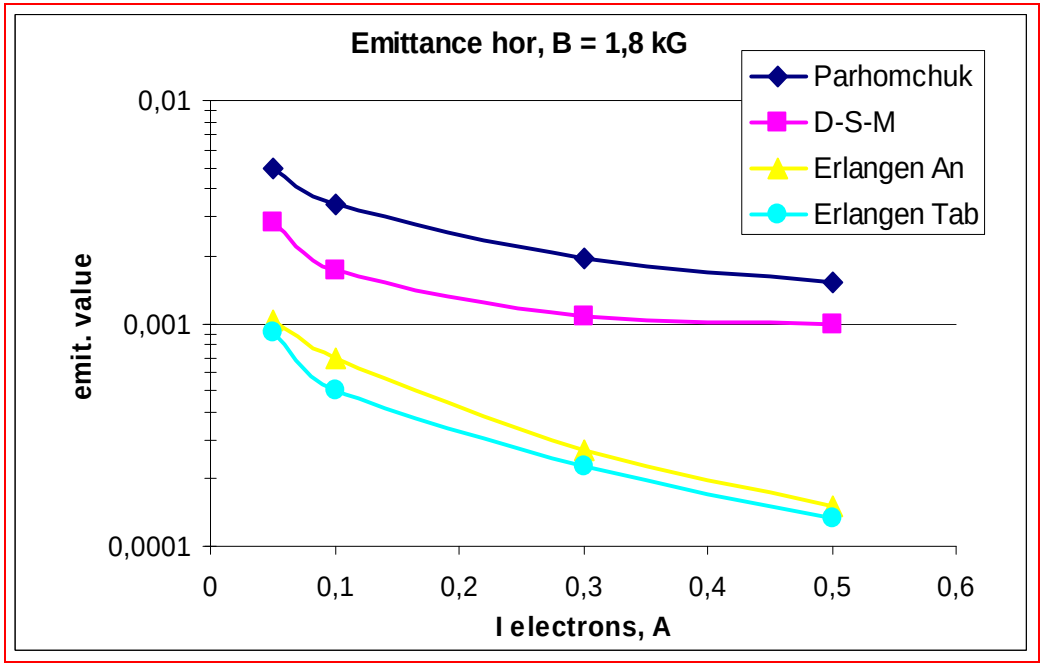
Emittance hor, B = 1,8 kG
Parhomchuk
D-S-M
Erlangen An
Erlangen Tab
emit. value
0,01
0,001
0,0001
0
0,1
0,2
0,3
0,4
0,5
0,6
I electrons, A

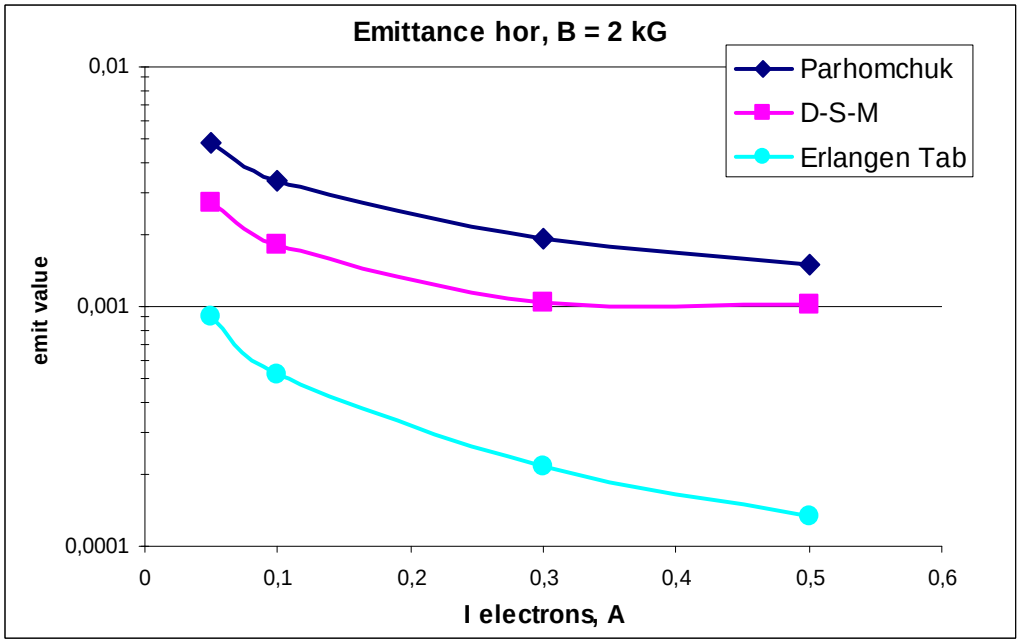
Emittance hor, B = 2 kG
Parhomchuk
D-S-M
Erlangen Tab
emit value
0,01
0,001
0,0001
0
0,1
0,2
0,3
0,4
0,5
0,6
I electrons, A

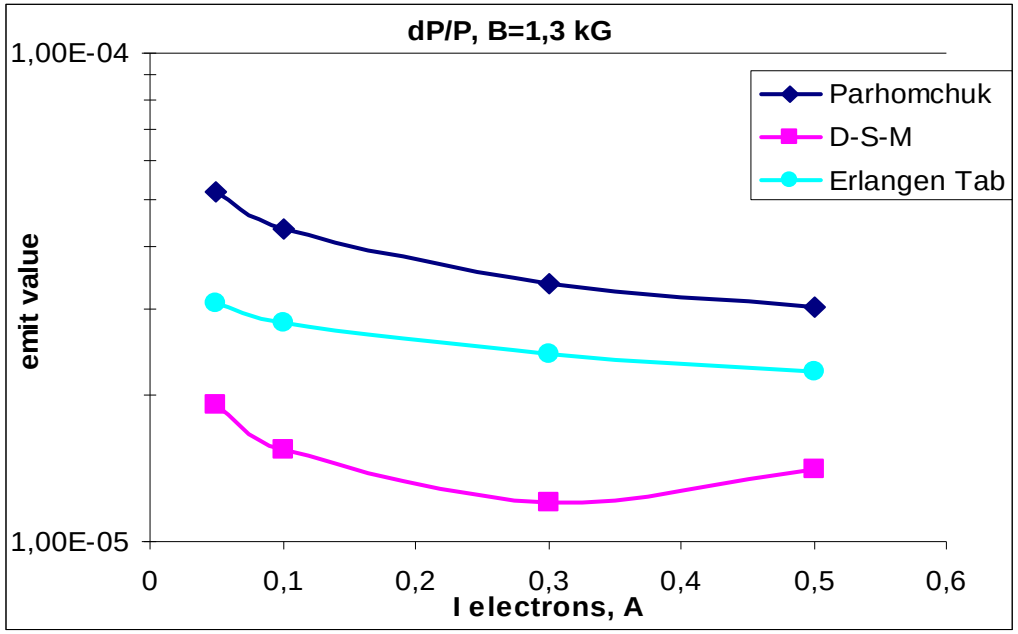
dP/P, B=1,3 kG
1,00E-04
1,00E-05
emit value
0
0,1
0,2
0,3
0,4
0,5
0,6
I electrons, A
Parhomchuk
D-S-M
Erlangen Tab

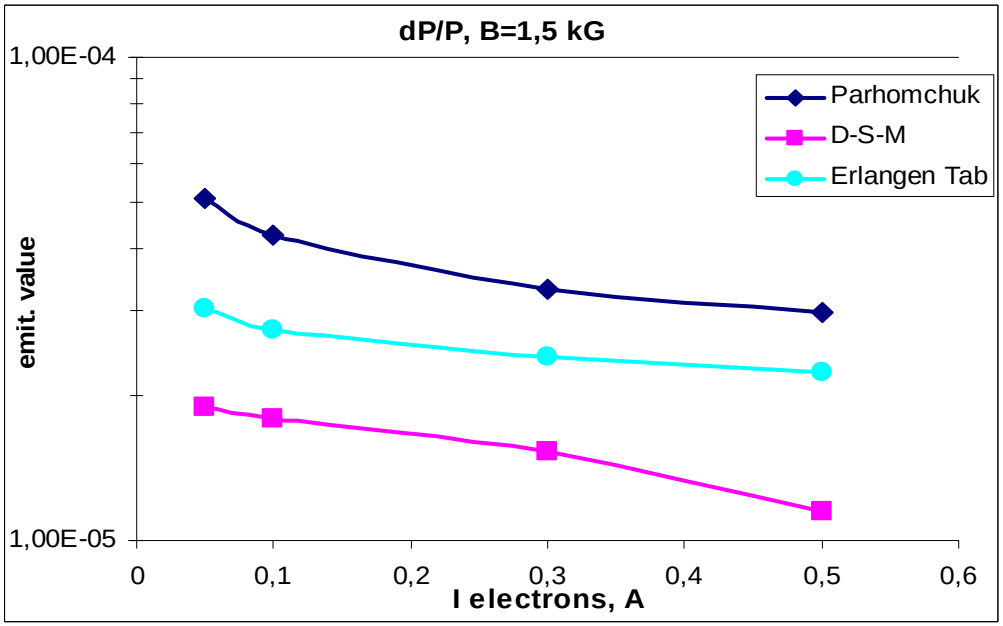
dP/P, B=1,5 kG
1,00E-04
1,00E-05
emit. value
0
0,1
0,2
0,3
0,4
0,5
0,6
I electrons, A
Parhomchuk
D-S-M
Erlangen Tab

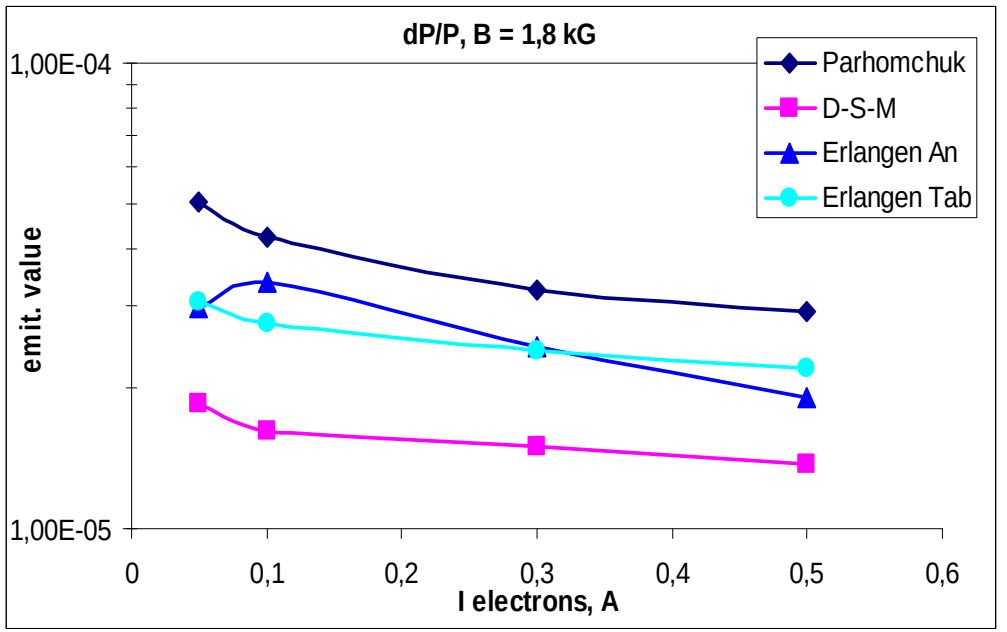
dP/P, B = 1,8 kG
1,00E-04
1,00E-05
emit. value
0
0,1
0,2
0,3
0,4
0,5
0,6
I electrons, A
Parhomchuk
D-S-M
Erlangen An
Erlangen Tab

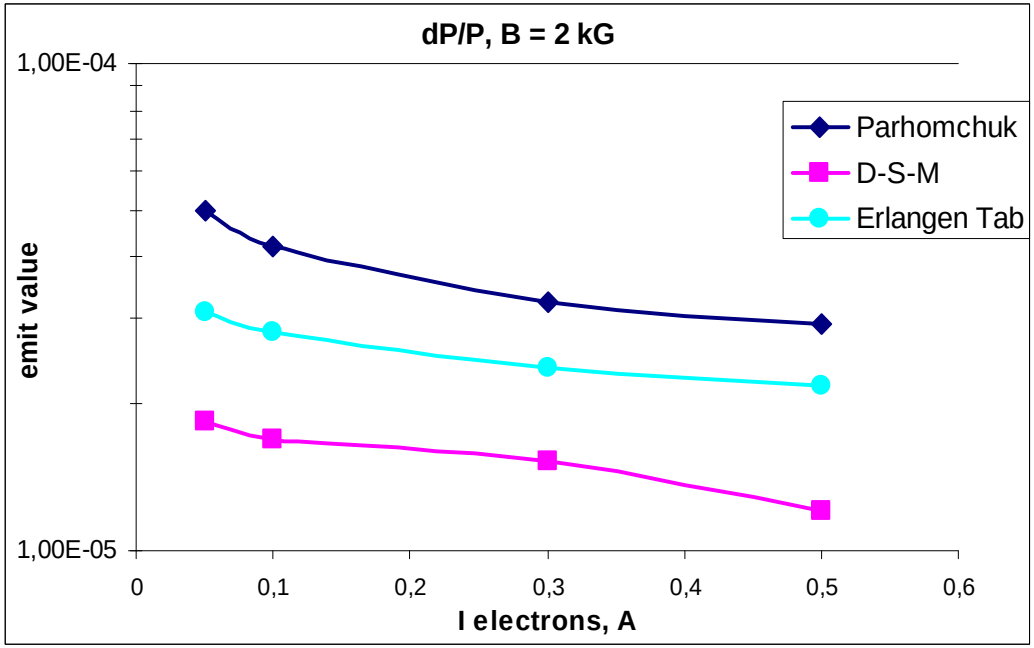
dP/P, B = 2 kG
1,00E-04
1,00E-05
emit value
0
0,1
0,2
0,3
0,4
0,5
0,6
I electrons, A
Parhomchuk
D-S-M
Erlangen Tab

2. MODELS OF ELECTRON BEAM

2.1 Hollow beam

Hollow beam is an infinite cylinder which has non-uniform radial density distribution. We assume in the code this model to be presented as two cylinders one inside another. Electron density is uniform inside each cylinder (Fig.2.1).

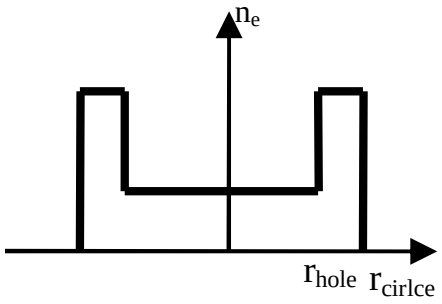

Fig.2.1. Electron density radial distribution in the hollow beam model.

The cross-section of such a beam is presented in the Fig. 2.2, where all the model input parameters are indicated.

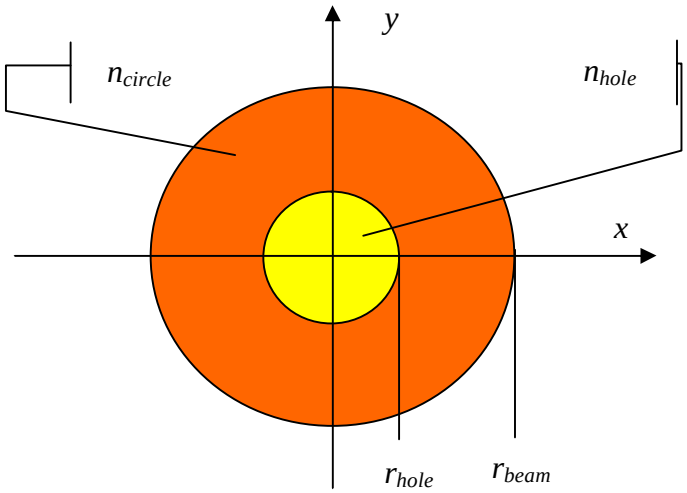

Fig.2.2. Cross-section of the hollow beam.

The input parameters are:

- the hole radius r_{hole},
- electron density in the laboratory rest frame (LRF) in the hole n_{hole},
- the outer circle radius r_{beam},
- density in LRF in the circle n_{circle}.

They are input in the visual form ECOOL | Electron beam in the tab sheet Hollow beam (Fig. 3) and are used to calculate the total beam current which is an output parameter.

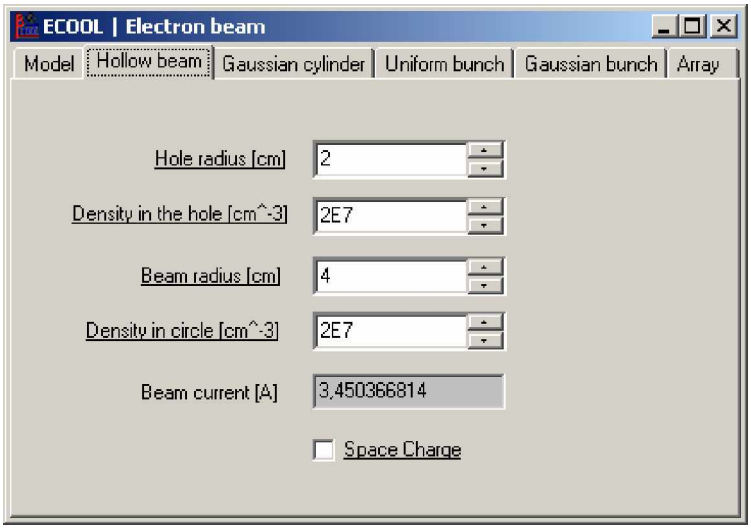

Fig. 2.3. Visual form for input and output the hollow beam parameters.

The beam current is calculated as

$$I_{beam} = I_{sum} + I_{hole} - I_{hole,n_{circle}}, \tag{2.1}$$

where I_{sum} is the current of the uniform cylinder at density equal to n_{circle}:

$$I_{sum} = en_{circle}\pi r_{beam}^2 \beta c, \tag{2.2}$$

I_{hole} is the current inside the hole:

$$I_{hole} = en_{hole}\pi r_{hole}^2 \beta c, \tag{2.3}$$

and $I_{hole,n_{circle}}$ is the current inside the hole at electron density equal to the density inside outer circle:

$$I_{hole,n_{circle}} = en_{circle}\pi r_{hole}^2 \beta c, \tag{2.4}$$

βc is the electron velocity.

In the current version of the program it is assumed that the electron thermal velocity spread has the same value inside the hole and in the outer circle.

Space charge effect in the hollow electron beam

The space charge effects lead to dependence of the mean electron velocity and electron velocity spread on co-ordinates inside the electron beam. There are two general effects related to the space charge of electron beam:

1. Electron longitudinal momentum shift due to potential distribution inside the beam,
2. Drift motion of the electrons in the crossed guiding longitudinal magnetic field of the cooler solenoid and radial electric field of the electron beam.

In difference with usual electron cooling system at the moment there is no realistic model of the beam neutralization by residual gas ions. For the electron beam at uniform density it was

experimentally proved at a few coolers, that the distribution of the residual gas ions inside the electron beam is closed to uniform. Therefore the space charge neutralization can be taken into account with analytical expressions for the beam self fields. For the hollow beam one can expect overcompensation of the electron space charge inside the hole and sufficiently non uniform ion distribution in the outer circle. To develop realistic model of the electron beam neutralization for the hollow beam detailed experimental investigations are necessary. Thus in the current version of the model the space charge effects can be taken into account correctly at zero neutralization degree only. The space charge effects are simulated in the program when the check box “Space Charge” (Fig. 2.3) is checked.

The electron momentum shift as a function of radial co-ordinate repeats the shape of potential distribution. It is assumed that at the beam axis the electron momentum corresponds to the ion one. In this case for instance in the electron beam at uniform distribution the shift in relative momentum is

$$\delta\theta_s = \frac{eI}{\beta^3 \gamma m_e c^3}\left(\frac{r}{a}\right)^2, \qquad (2.5)$$

where I is the beam current and a – its radius.

For the hollow beam the potential distribution can be found as a superposition of potentials of two beams: negatively charged beam at density n_{circle} and radius r_{beam} and positively charged beam at density $n_{circle} - n_{hole}$ and radius r_{hole} (Fig. 2.4).

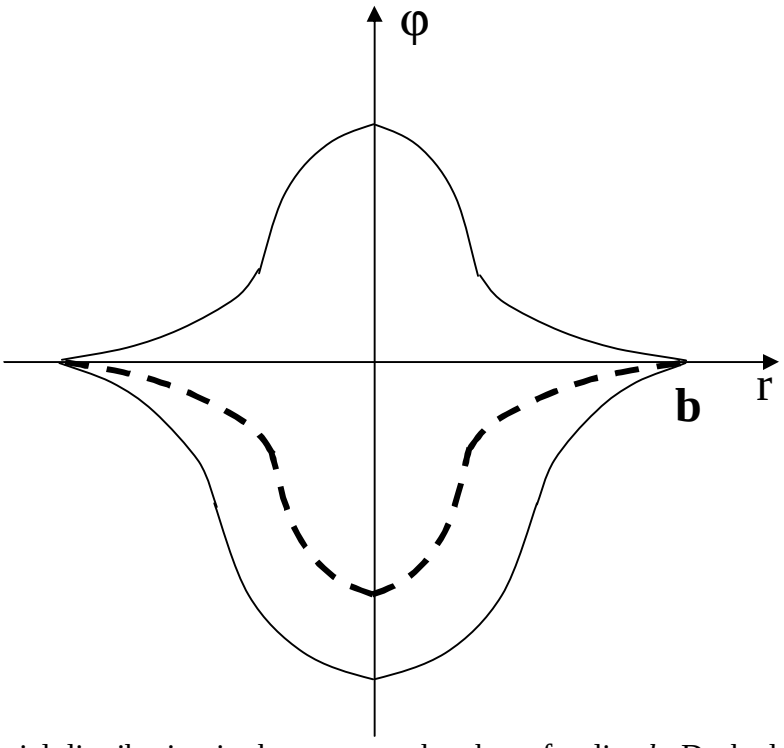

Fig. 2.4. The potential distribution in the vacuum chamber of radius *b*. Dashed line corresponds to potential distribution of the hollow beam.

The relative momentum shift in the negatively charged beam is given by the same formula (5). The potential distribution of the positively charged beam (under assumption that the potential at the beam axis is zero) is given by the formula:

$$\varphi(r) = -\frac{I}{\beta c}\begin{cases} \dfrac{r^2}{r_{hole}^2}, & 0 < r \le r_{hole} \\ 1 + 2\ln\dfrac{b}{r_{hole}} - 2\ln\dfrac{b}{r}, & r > r_{hole} \end{cases}, \tag{2.6}$$

where the beam current is calculated as

$$I = e(n_{circle} - n_{hole})\pi r_{hole}^2 \beta c\,. \tag{2.7}$$

The relative coherent drift velocity (drift angle) for uniform cylinder is calculated as:

$$\theta_d = \frac{2I}{cB\beta\gamma^2}\frac{r}{a^2}, \tag{2.8}$$

where *B* is the magnetic field value. The electric field in this formula is obtained as a derivative of the beam potential. In the case of hollow beam the drift angle is a linear function of the radial co-ordinate inside the hole, and superposition of linear and inversely proportional functions in the outer circle. For the space charge simulation in the hollow beam an additional input parameter is required – the vacuum chamber radius in the cooler.

3. INTERNAL TARGET MODEL
3.1. The simulations of the ESR experiments.

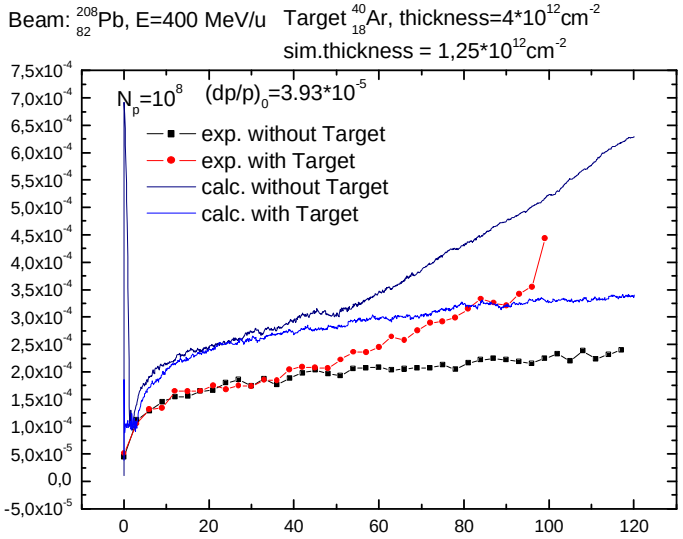

The experimental results for the time evolution of Δp/p and Ex,y without target and with Ar target (d=4E12atom/cm^2) are shown in comparison a BetaCool simulation made under similar conditions as in experiment. In the simulation? The Martini model is used for IBS, the Parkhomchuk formula for the cooling forces and the fiber model of the target with density = 1.25E12atom/cm^2. The optimum d_{sim} is ~25% of d and this is just the geometrical beam-jet overlap factor. For the relative blow-up of Δp/p the agreement is excellent. As for Ex,y we have disagreement between measurements and simulations.

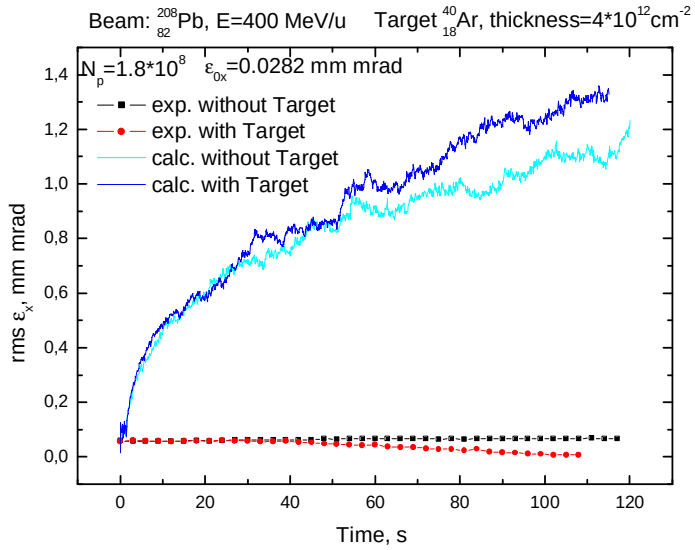

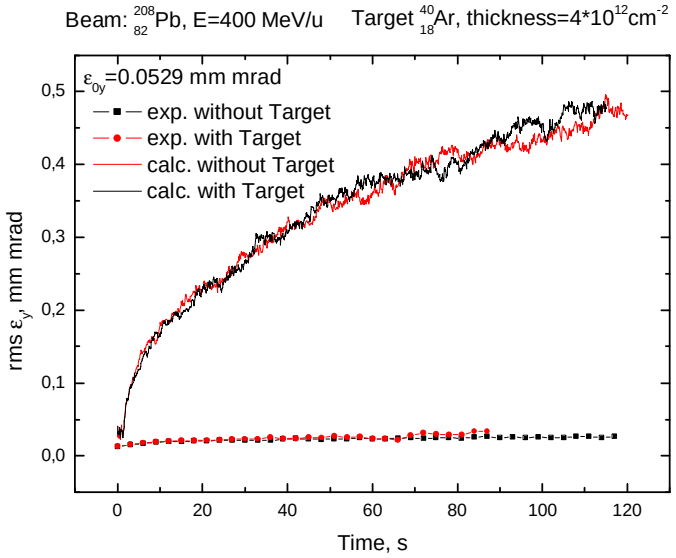

3.2. The simulations of the future NESR experiments.

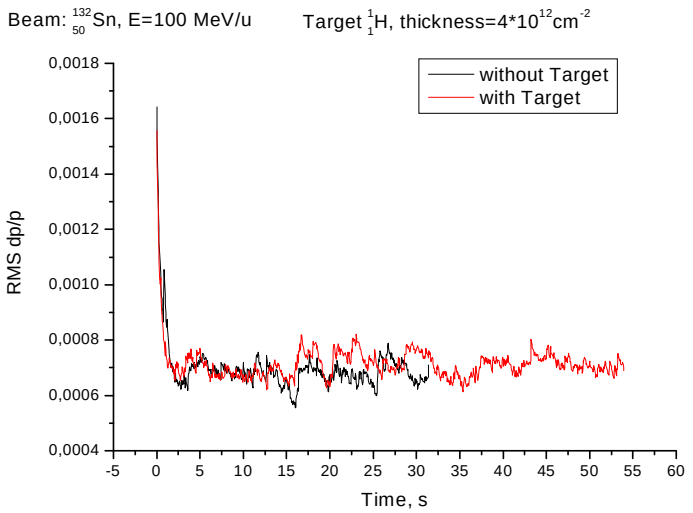

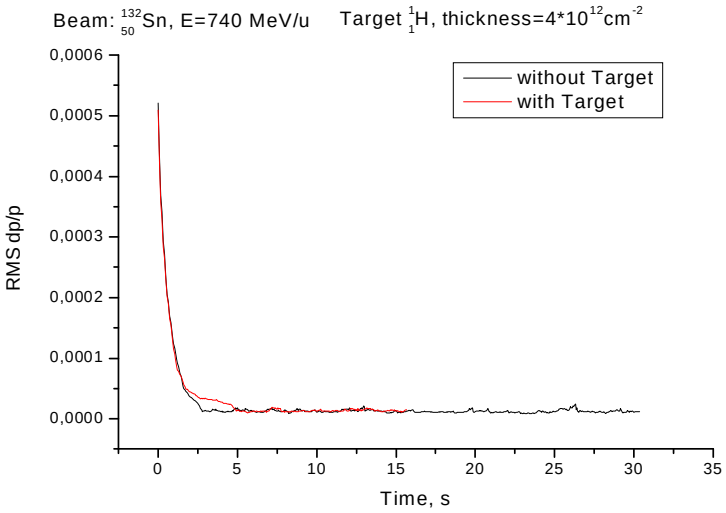

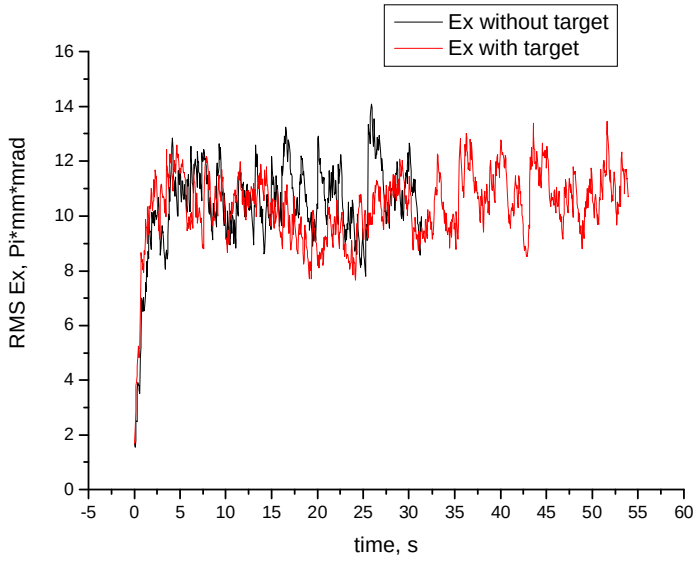

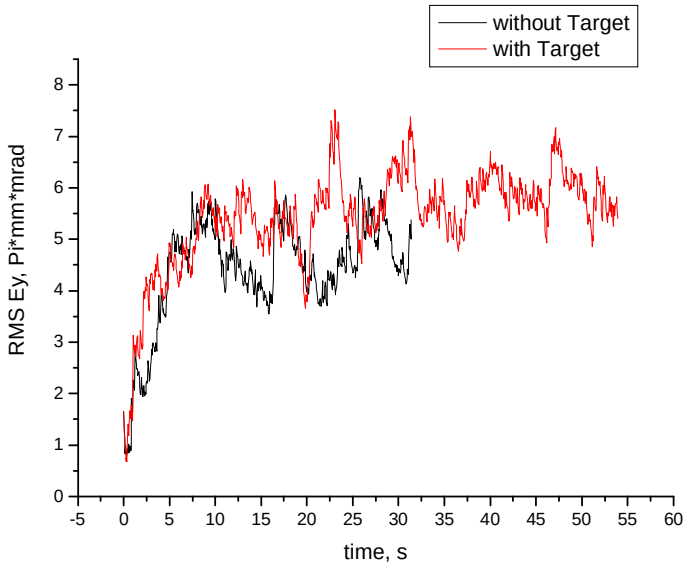

4. SIMULATION OF KINETIC IBS WITH MODEL BEAM

4.1. Kinetic model of IBS on the basis of Bjorken-Mtingwa theory

Kinetic simulation of IBS process presumes a solution of Langevin equation for each model particle. The drift and diffusion terms of the equation has to be calculated for each particle independently as a function of its co-ordinates, velocity components and distribution function of all other particles in the Model Beam.

To benchmark the algorithm reducing friction and diffusion to Langevin force components the simplified kinetic model for IBS simulation proposed by P.Zenkevich and O.Boine-Frankenheim was introduced into the code and tested preliminary at parameters typical for gold-gold collisions at RHIC. This model is based on analytical formulae for friction and diffusion components and presumes that only the friction depends on the particle velocity. The diffusion tensor in the frame of this model does not depend on the particle momentum and has a simplified structure.

Accurate benchmarking the code presumes simulation of IBS process at different lattice structures and at different parameters of the ion distribution function. For instance, RHIC is operated over transition energy and longitudinal temperature of the ion bunch is sufficiently less than transverse one. At these conditions the growth of the phase volume of the bunch is determined by longitudinal diffusion mainly. All other terms (friction and transverse diffusion components) are less as minimum by about one order of magnitude. Therefore the obtained good coincidence of the kinetic simulations with rms dynamics predictions for RHIC parameters indicates that the D_{zz} component of the diffusion tensor are calculated correctly and overall algorithm structure was developed properly. To benchmark all the parts of the code one needs to provide simulations below transition (or as for HESR – at imaginary transition energy) at bunch parameters closed to thermal equilibrium, which permits to test other components of the diffusion tensor. The friction force plays a leading role in the relaxation process. Therefore the benchmarking of this part of algorithm presumes simulation of IBS process for a bunch at sufficiently different temperatures of different degrees of freedom. It is preferable to perform the simulations for a ring working below transition energy (for instance, NESR).

Another effect which has to be taken into account by the kinetic IBS model is residual coupling between transverse degrees of freedom. In the frame of rms dynamics model the simulations are providing at the following assumptions:

- during single revolution of the beam in the ring the coupling can be neglected, and IBS growth rates are calculated in accordance with uncoupled ring lattice structure;
- at a long step of integration over time the residual coupling leads to equality of the horizontal and vertical growth rates:

$$\frac{1}{\tau_{x,coupled}} = \frac{1}{\tau_{y,coupled}} = \frac{1}{2}\left(\frac{1}{\tau_x} + \frac{1}{\tau_y}\right)_{uncoupled}.$$

In the frame of the kinetic model motion of each model particle is simulated depending on its momentum components, correspondingly the mean heating rates can not be used for the simulations directly. The long term coupling in this case can be simulated as a beam rotation in the (x, y) plane at some angle after each integration step. Simplest version of this algorithm was realized in the code, it requires further development and an accurate benchmarking.

In the frame of Bjorken-Mtingwa model of BETACOOL program the IBS growth rates are calculated in accordance with:

$$\begin{cases} \dfrac{1}{\tau_x} = \left\langle \dfrac{\mathrm{H}_x}{\varepsilon_x}\gamma_0^2 I_{zz} - 2\dfrac{\beta_x\phi_{Bx}}{\varepsilon_x}\gamma_0 I_{xz} + \dfrac{\beta_x}{\varepsilon_x} I_{xx} \right\rangle_s \\ \dfrac{1}{\tau_y} = \left\langle \dfrac{\mathrm{H}_y}{\varepsilon_y}\gamma_0^2 I_{zz} - 2\dfrac{\beta_y\phi_{By}}{\varepsilon_y}\gamma_0 I_{yz} + \dfrac{\beta_y}{\varepsilon_y} I_{yy} \right\rangle_s \\ \dfrac{1}{\tau_z} = \left\langle \dfrac{1}{2}\dfrac{\gamma_0^2}{\sigma_p^2} I_{zz} \right\rangle_s \end{cases}, \qquad (4.1)$$

where $\phi_{Bi} = D_i^{/} + \alpha_i D_i / \beta_i$, $\mathrm{H}_i = \beta_i D_i'^2 + 2\alpha_i D_i D_i^{/} + \gamma D_i^2$ and $\alpha_i, \beta_i, \gamma_i$ - lattice functions in the horizontal ($i=x$) and vertical ($i=y$) plane, $\varepsilon_{x,y}$ are the horizontal and vertical emittances, σ_p – rms momentum spread. Angular brackets mean averaging over the ring circumference. This modification of Bjorken-Mtingwa theory was proposed by Venturini to tacke into account residual vertical dispersion in the storage ring.

The collision coefficients I_{ij} are calculated in each position of the ring by numerical evaluation of the following integrals

$$I_{ij} \equiv \frac{d\left(P_i P_j\right)}{dt} = A\int_0^\infty d\lambda \frac{\lambda^{1/2}}{\sqrt{\det\Lambda}}\left(\delta_{ij} Tr\Lambda^{-1} - 3\Lambda_{ij}^{-1}\right), \qquad (4.2)$$

where the matrix $\Lambda = I\lambda + L$, I – unit matrix, and matrix L is calculated via beam rms parameters and ring lattice functions in accordance with:

$$L = \begin{bmatrix} \dfrac{\beta_x}{\varepsilon_x} & 0 & -\gamma_0\dfrac{\beta_x\phi_{Bx}}{\varepsilon_x} \\ 0 & \dfrac{\beta_y}{\varepsilon_y} & -\gamma_0\dfrac{\beta_y\phi_{By}}{\varepsilon_y} \\ -\gamma_0\dfrac{\beta_x\phi_{Bx}}{\varepsilon_x} & -\gamma_0\dfrac{\beta_y\phi_{By}}{\varepsilon_y} & \dfrac{\gamma_0^2\mathrm{H}_x}{\varepsilon_x} + \dfrac{\gamma_0^2\mathrm{H}_y}{\varepsilon_y} + \dfrac{\gamma_0^2}{\sigma_p^2} \end{bmatrix}, \qquad (4.3)$$

The IBS constant A is determined as in other IBS models:

$$A = \frac{c r_i^2 N L_c}{8\pi\beta^3\gamma_0^2\varepsilon_x\varepsilon_y\sigma_p\sigma_s}. \qquad (4.4)$$

Here β and γ_0 are the Lorenz parameters, r_i is the ion classical radius, N is the ion number, L_c is the Coulomb logarithm, which is introduced as an input parameter.

At ion distribution function closed to Gaussian one the kinetic simulation of IBS process in the frame of Model Beam algorithm is realized on the basis of the following simplifications:

- the components of the friction force are a linear functions of the ion momentum $F_i = -K_i P_i$, where K_i are the constants,
- the components of the diffusion tensor $D_{i,j}$ do not depend on the ion momentum.

The model particle momentum variation after crossing an optic element of length l_k are calculated in accordance with Langevin equation:

$$P_i(t+\Delta t) = P_i(t) - K_i P_i(t)\Delta t \frac{l_k}{C} + \sqrt{\Delta t \frac{l_k}{C}} \sum_{j=1}^{3} C_{i,j}\xi_j \,, \tag{4.5}$$

where ξ_j are three Gaussian random numbers with unit dispersion. The coefficients $C_{i,j}$ have to be calculated from diffusion and friction coefficients. Total momentum variation is calculated in cycle over optic elements along the ring circumference C.

The diffusion tensor men components in the frame of Bjorken –Mtingwa model are calculated as the following integrals:

$$D_{i,j} = A\int_0^\infty d\lambda \frac{\lambda^{1/2}}{\sqrt{\det \Lambda}} (\delta_{ij} Tr\Lambda^{-1} - \Lambda_{ij}^{-1}) \,. \tag{4.6}$$

The collision coefficients can be expressed via friction and diffusion components as follows:

$$\left\langle \frac{d(P_i P_j)}{dt} \right\rangle = -(K_i + K_j)\langle P_i P_j \rangle + D_{i,j} \,, \tag{4.7}$$

where triangular brackets mean averaging over the particles. $\delta_{i,j}$ is the Kronecker-Kapelli symbol.

Comparing (4.2) and (4.7) one can find expressions for the friction coefficients:

$$K_i = \frac{A}{\langle P_i^2 \rangle} \int_0^\infty d\lambda \frac{\lambda^{1/2}}{\sqrt{\det \Lambda}} \Lambda_{ii}^{-1} \,. \tag{4.8}$$

To find expressions for $C_{i,j}$ lets multiply the momentum variation for i and j-th particles:

$$P_i(t+\Delta t)P_j(t+\Delta t) = \left(P_i(t) - K_i P_i(t)\Delta t + \sqrt{\Delta t}\sum_{k=1}^{3} C_{i,k}\xi_k \right)\left(P_j(t) - K_j P_j(t)\Delta t + \sqrt{\Delta t}\sum_{k=1}^{3} C_{j,k}\xi_k \right) =$$

$$= P_i(t)P_j(t) - (K_i + K_j)P_i(t)P_j(t)\Delta t + K_i K_j P_i(t)P_j(t)(\Delta t)^2 + P_i(t)\sqrt{\Delta t}\sum_{k=1}^{3} C_{j,k}\xi_k +$$

$$+ P_j(t)\sqrt{\Delta t}\sum_{k=1}^{3} C_{i,k}\xi_k + \sum_{k=1}^{3} C_{i,k}\xi_k \sum_{k=1}^{3} C_{j,k}\xi_k \Delta t$$

and average this expression over the particles. Neglecting the term $(\Delta t)^2$ and taking into account that

$$\left\langle P_j(t)\sqrt{\Delta t}\sum_{k=1}^{3} C_{i,k}\xi_k \right\rangle = 0 \,,$$

$$\langle \xi_i \xi_j \rangle = \delta_{i,j} \,,$$

we obtain

$$\frac{\langle \Delta P_i P_j \rangle}{\Delta t} = -(K_i + K_j)\langle P_i P_j \rangle + \sum_{k=1}^{3} C_{i,k} C_{j,k} \,. \tag{4.9}$$

The coefficients $C_{i,k}$ have to be chosen to obtain the same values of collision integrals (4.7), that gives the following system of equations:

$$-(K_i + K_j)\langle P_i P_j \rangle + \sum_{k=1}^{3} C_{i,k} C_{j,k} = -(K_i + K_j)\langle P_i P_j \rangle + D_{i,j} \,. \tag{4.10}$$

Due to diagonal symmetry of the diffusion tensor the system consists of the following 6 independent equations for 9 unknown coefficients:

$$\begin{gathered} C_{x,1}C_{y,1} + C_{x,2}C_{y,2} + C_{x,3}C_{y,3} = D_{x,y} \\ C_{x,1}C_{z,1} + C_{x,2}C_{z,2} + C_{x,3}C_{z,3} = D_{x,z} \\ C_{y,1}C_{z,1} + C_{y,2}C_{z,2} + C_{y,3}C_{z,3} = D_{y,z} \\ C_{x,1}^2 + C_{x,2}^2 + C_{x,3}^2 = D_{x,x} \\ C_{y,1}^2 + C_{y,2}^2 + C_{y,3}^2 = D_{y,y} \\ C_{z,1}^2 + C_{z,2}^2 + C_{z,3}^2 = D_{z,z} \end{gathered} \tag{4.11}$$

This system has an infinite number of solutions and can be simplified, when the diffusion tensor has a zero components. In our case $D_{x,y} = 0$ and $\langle P_x P_y \rangle = 0$, the solution can be build by the following way. Lets assume, that the random number ξ_1 correspond to scattering in horizontal plane, ξ_2 – in vertical and put $C_{x,2} = C_{y,1} = 0$. From the first equation of the system (4.10) follows that $C_{x,3}C_{y,3} = 0$. Lets put $C_{x,3} = 0$. In this case

$$C_{x,1} = \sqrt{D_{x,x}} \,. \tag{4.12}$$

From the second equation of (4.10) follows

$$C_{z,1} = \frac{D_{x,z}}{\sqrt{D_{x,x}}} \,. \tag{4.13}$$

Then, for simplicity put

$$C_{y,2} = C_{y,3} = \sqrt{D_{y,y}/2} \,. \tag{4.14}$$

From the third equation of (4.10):

$$C_{z,2} = \frac{D_{y,z}}{\sqrt{D_{y,y}/2}} - C_{z,3} \,. \tag{5.15}$$

Substituting (4.13) and (4.15) into the last equation of (4.10) we obtain quadratic equation about $C_{z,3}$:

$$C_{z,3}^2 - \frac{D_{y,z}}{\sqrt{D_{y,y}/2}} C_{z,3} + \frac{\left(D_{x,z}\right)^2}{2D_{x,x}} + \frac{\left(D_{y,z}\right)^2}{D_{y,y}} - \frac{D_{z,z}}{2} = 0 .$$

In absence of vertical dispersion ($D_{y,z} = 0$, $\left\langle P_y P_z \right\rangle = 0$) it gives

$$C_{z,3} = \sqrt{\frac{D_{z,z}}{2} - \frac{\left(D_{x,z}\right)^2}{2D_{x,x}}} . \tag{4.16}$$

In the general case

$$C_{z,3} = \frac{D_{y,z}}{\sqrt{2D_{y,y}}} \pm \sqrt{\frac{D_{z,z}}{2} - \frac{\left(D_{x,z}\right)^2}{2D_{x,x}} - \frac{\left(D_{y,z}\right)^2}{2D_{y,y}}} . \tag{4.17}$$

Fixing the sign plus in the last expression one can write total set of the coefficients:

$$\begin{aligned}
C_{x,1} &= \sqrt{D_{x,x}} , \\
C_{y,2} &= C_{y,3} = \sqrt{D_{y,y}/2} , \\
C_{z,1} &= \frac{D_{x,z}}{\sqrt{D_{x,x}}} , \\
C_{z,2} &= \frac{D_{y,z}}{\sqrt{D_{y,y}/2}} - \sqrt{\frac{DetD}{2D_{x,x}D_{y,y}}} , \\
C_{z,3} &= \frac{D_{y,z}}{\sqrt{2D_{y,y}}} + \sqrt{\frac{DetD}{2D_{x,x}D_{y,y}}} ,
\end{aligned} \tag{4.18}$$

all the other are equal to zero. Here *DetD* is the determinant of the matrix

$$\begin{pmatrix}
D_{x,x} & 0 & D_{x,z} \\
0 & D_{y,y} & D_{y,z} \\
D_{x,z} & D_{y,z} & D_{z,z}
\end{pmatrix}, \tag{4.19}$$

$D_{i,j}$ are calculated in accordance with (5.6).

Taking into account that the diffusion and friction components are determined for the following momentum components:

$$\left(x' - D_x' \frac{\Delta p}{p}, y' - D_y' \frac{\Delta p}{p}, \frac{1}{\gamma} \frac{\Delta p}{p} \right), \tag{4.20}$$

the variations of the ion momentum components inside *k*-th optic element are given by

$$\Delta x_n^{/} = -F_x \frac{\left(x_n^{/} - D_x^{/} \frac{\Delta p}{p}_n \right) \beta_{x,k}}{\varepsilon_x \left(1+\alpha_{x,k}^2\right)} \Delta t \frac{l_k}{C} + \sqrt{D_{x,x} \Delta t \frac{l_k}{C}} \xi_1, \qquad (4.21)$$

$$\Delta y_n^{/} = -F_y \frac{\left(y_n^{/} - D_y^{/} \frac{\Delta p}{p}_n \right) \beta_{y,k}}{\varepsilon_y \left(1+\alpha_{x,k}^2\right)} \Delta t \frac{l_k}{C} + \sqrt{\frac{D_{y,y}}{2} \Delta t \frac{l_k}{C}} \xi_1 + \sqrt{\frac{D_{y,y}}{2} \Delta t \frac{l_k}{C}} \xi_2, \qquad (4.22)$$

$$\Delta \frac{\Delta p}{p_n} = -F_z \frac{\gamma \frac{\Delta p}{p}_n}{\varepsilon_{long}} \Delta t \frac{l_k}{C} + \sqrt{\Delta t \frac{l_k}{C}} \gamma C_{z,1} \xi_1 + \sqrt{\Delta t \frac{l_k}{C}} \gamma C_{z,2} \xi_2 + \sqrt{\Delta t \frac{l_k}{C}} \gamma C_{z,3} \xi_3, \qquad (4.23)$$

here n is the number of the particle, $\varepsilon_{x,y}$ – horizontal and vertical emittances, α_k, β_k, $D_k^{/}$ - lattice parameters, longitudinal emittance is determined as $\varepsilon_{long} = \sigma_p^2$, γ is Lorenz factor, the friction coefficients F_i are calculated in accordance with:

$$F_{x,y} = \frac{\beta_{x,y}}{\varepsilon_{x,y}\left(1+\alpha_{x,y}^2\right)} A \int_0^\infty d\lambda \frac{\lambda^{1/2}}{\sqrt{\det \Lambda}} \Lambda_{ii}^{-1}, \qquad (4.24)$$

$$F_z = \frac{1}{\varepsilon_{long}} A \int_0^\infty d\lambda \frac{\lambda^{1/2}}{\sqrt{\det \Lambda}} \Lambda_{ii}^{-1}. \qquad (4.25)$$

To test a possibility to simulate the IBS process in presence of a residual coupling between transverse planes the simplest algorithm was implemented into program. After each step of integration over time the beam is rotated by 90^0 around longitudinal axis. For each particle its co-ordinates are changed in accordance with the following equation:

$$\begin{pmatrix} x \\ y \end{pmatrix} = \begin{pmatrix} 0 & -1 \\ 1 & 0 \end{pmatrix} \begin{pmatrix} x \\ y \end{pmatrix}_0. \qquad (4.26)$$

For Gaussian distribution the described kinetic model has to coincide with Rms dynamics simulation using Bjorken-Mtingwa model. Comparison of the kinetic model and Rms dynamics simulations are presented in the Fig. 4.1, 4.2. The simulations were performed at RHIC parameters, corresponding to gold-gold collisions at 100 GeV/u.

Even at model particle number of 2000 the coincidence is satisfactory. The simulations were provided at ideal RHIC lattice and the vertical dispersion was assumed to be zero along the total ring circumference. At the typical gold bunch parameters (rms emittance of about $2.5 \cdot 10^{-8}$ π·m·rad in both planes and rms momentum spread of $5 \cdot 10^{-4}$) general term determining the IBS growth is z-z component of the diffusion tensor. The friction and other components of the diffusion are negligible in comparison with mistakes of the simulations. Therefore the collision integral consists of only one significant term – I_{zz}, which coinsides practically with the corresponding diffusion component. At uncoupled motion, in accordance with (4.1) the I_{zz} component determines the momentum spread and horizontal emittance growth. At absence of vertical diffusion the vertical emittance growth rate is determined by I_{yy} component of the collision integral and from Fig. 4.1 ne can see that this component is comparable with the noise of the algorithm. The I_{xx} and I_{xz} have the

same order of magnitude as I_{yy} and the horizontal emittance growth is caused by the longitudinal diffusion mainly.

4.2. Benchmarking

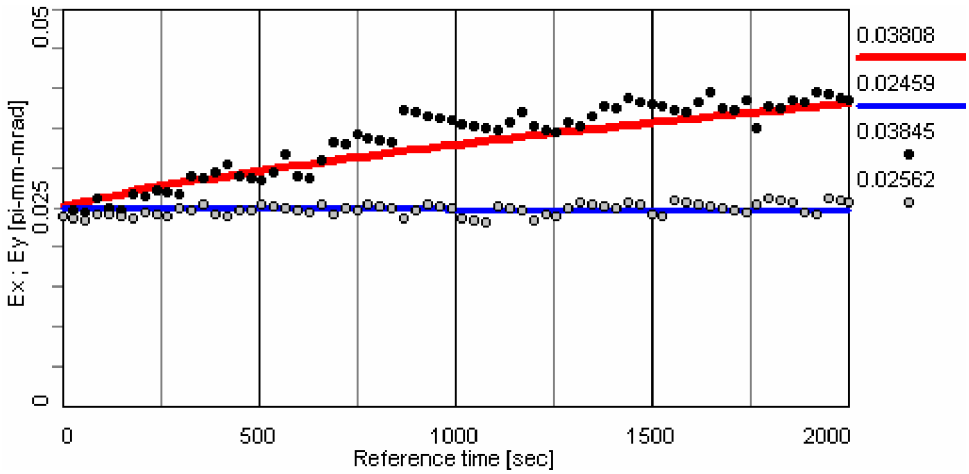

Fig. 4.1. Horizontal emittance time dependence. RMS dynamics – read solid line, kinetic model (2000 particles) – black dots. Vertical emittance time dependence. RMS dynamics – blue solid line, kinetic model (2000 particles) – gray dots.

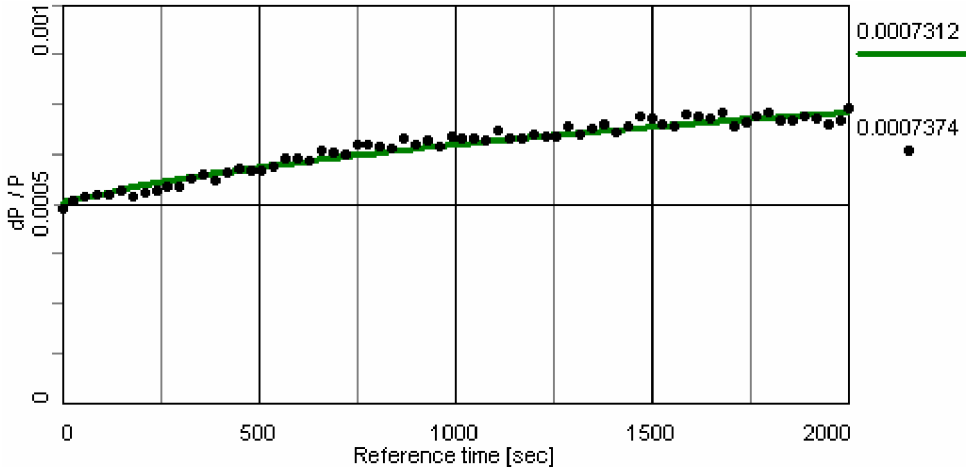

Fig. 4.2. Momentum spread time dependence. RMS dynamics solid line, kinetic model (2000 particles) – black dots.

Good agreement of the momentum spread evolution (Fig. 4.2) between exact theory result and kinetic model indicates that the diffusion due to the componet D_{zz} is simulated correctly. Good agreement in the horizontal emittance evolution indicates that the algorithm structure is built correctly. All other components of the collision integral are calculated correctly by the order of magnitude (as minimum they are not overestimated) that leads to very small variation of vertical emittance in time (Fig. 4.1). Accurate benchmarking the algorithm requires more extensive simulations in a wide range of a storage ring and beam parameters. This work we plan to provide at the next stage of JINR – GSI cooperation.

5. THE IMPROVEMENT OF THE BETACOOL INTERFACE IN ACCORDANCE WITH GSI REQUIREMENTS.

Red colour – removed
Green – changed
Black – unchanged

Beam

- **Parameters**
- **Distribution**
- **Evolution**
- **Real Space**
- **Colliding Beam**

Ring

- **Parameters**
- **Lattice Structure**

Task

- **Growth Rates**
- **Parameters**
- **RMS Dynamics**
- **Model Beam**
- **Tracking**

Effects

- **Rest Gas**
- **Internal target**
- **Collision Point**
- **Particle Losses**
- **Intrabeam Scattering**
- **Additional Heating**
- **Stochastic Cooling**
- **Optical Stoch. Cooling**
- **Laser Cooling**

ECOOL

- **Tabulated**
- **Cooler**
- **Electron beam**
- **Friction force**
- **Draw forces**